Ann Nucl Med (2016) 30:122–129
DOI 10.1007/s12149-015-1039-6

ORIGINAL ARTICLE

Synthesis and evaluation of a new vesamicol analog *o*-[^{11}C]methyl-*trans*-decalinvesamicol as a PET ligand for the vesicular acetylcholine transporter

Yoji Kitamura[1] · Takashi Kozaka[1] · Daisuke Miwa[1] · Izumi Uno[1,2] · Mohammad Anwar-ul Azim[3] · Kazuma Ogawa[2] · Junichi Taki[2] · Seigo Kinuya[2] · Kazuhiro Shiba[1]

Received: 8 July 2015 / Accepted: 8 November 2015 / Published online: 25 November 2015

Abstract
Introduction We focused on the vesicle acetyl choline transporter (VAChT) as target for early diagnosis of Alzheimer's diseases because the dysfunction of the cholinergic nervous system is closely associated with the symptoms of AD, such as problem in recognition, memory, and learning. Due to its low binding affinity for the sigma receptors (σ-1 and σ-2), *o*-methyl-*trans*-decalinvesamicol (OMDV) demonstrated a high binding affinity and selectivity for vesicular acetyl choline transporter (VAChT). [^{11}C]OMDV was prepared and investigated the potential as a new PET ligand for VAChT imaging through in vivo evaluation.
Method [^{11}C]OMDV was prepared by a palladium-promoted cross-coupling reaction using [^{11}C]methyl iodide, with a radiochemical yield of 60–75 %, a radiochemical purity of greater than 98 %, and a specific activity of 5–10 TBq/mmol 30 min after EOB. In vivo biodistribution study of [^{11}C]OMDV in blood, brain regions and major organs of rats was performed at 2, 10, 30 and 60 min post-injection. In vivo blocking study and PET–CT imaging study were performed to check the binding selectivity of [^{11}C]OMDV for VAChT.
Results In vivo studies demonstrated [^{11}C]OMDV passage through the blood–brain barrier (BBB) and accumulation in the rat brain. The regional brain accumulation of [^{11}C]OMDV was significantly inhibited by co-administration of vesamicol. In contrast, brain accumulation of [^{11}C]OMDV was not significantly altered by co-administration of (+)-pentazocine, a selective σ-1 receptor ligand, or (+)-3-(3-hydroxyphenyl)-*N*-propylpiperidine [(+)-3-PPP], a σ-1 and σ-2 receptor ligand. PET–CT imaging revealed inhibition of [^{11}C]OMDV accumulation in the brain by co-administration of vesamicol.
Conclusion [^{11}C]OMDV selectively binds to VAChT with high affinity in the rat brain in vivo, and that [^{11}C]OMDV may be utilized in the future as a specific VAChT ligand for PET imaging.

Keywords PET · Vesamicol analogs · Vesicular acetylcholine transporter · Presynaptic cholinergic neurons

✉ Yoji Kitamura
ykitamu@staff.kanazawa-u.ac.jp

✉ Takashi Kozaka
t-kozaka@staff.kanazawa-u.ac.jp

✉ Kazuhiro Shiba
shiba@med.kanazawa-u.ac.jp

[1] Division of Tracer Kinetics, Advanced Science Research Center, Kanazawa University, 13-1 Takara-machi, Kanazawa, Ishikawa 920-8640, Japan

[2] Institute of Medical, Pharmaceutical and Health Sciences, Kanazawa University, 13-1 Takara-machi, Kanazawa, Ishikawa 920-8640, Japan

[3] National Institute of Nuclear Medicine and Allied Sciences, Bangladesh Atomic Energy Commission, BSM Medical University Campus, Block-D, 7th-10th floor, Shahbagh, Dhaka 1000, Bangladesh

Introduction

Acetylcholine esterase inhibitors are commonly used for treatment of cognitive dysfunction in Alzheimer's disease (AD) [1, 2]. The dysfunction of the cholinergic nervous system is closely associated with the symptoms of AD, such as problem in recognition, memory, and learning. In AD, decreases in presynaptic cholinergic functions, such as choline acetyl transferase (ChAT) [3, 4] and VAChT [5–7]

activity, is thought to be more significant than changes in postsynaptic cholinergic functions. VAChT, which transports ACh into synaptic vesicles, is a known cholinergic neuron terminal marker [8]. Loss of synapses and synaptic dysfunction occurs prior to fibrillary tau tangle emergence in tauopathy model mice, a type of AD model [9]. Therefore, VAChT may be an excellent in vivo target substrate for the diagnosis of AD.

Because vesamicol (2-(4-phenylpiperidino)cyclohexanol) was reported to bind to VAChT [10, 11], many radiolabeled vesamicol analogs have been investigated as potential VAChT imaging ligands for use in PET or SPECT imaging [12–18]. However, many of the reported vesamicol analogs were shown to be insufficient for use as VAChT imaging ligands, due to also binding to sigma receptors (σ-1 and σ-2) [19]. Rogers et al. reported that *trans*-decalinvesamicol (DV) had the highest affinity for VAChT among 84 vesamicol analogs in an in vitro binding assay [20]. However, the chemical structure of DV was unsuitable for introduction of a radionuclide such as radioiodine or ^{11}C. We reported several radiolabeled vesamicol analogs in which radioiodine or a [^{11}C]methyl group at the *ortho*-position of the 4-phenylpiperidine moiety was introduced (radioiodinated oIV [17], [^{11}C]OMV). We designed a DV compound with halogen or methyl group at the *ortho*-position of the 4-phenylpiperidine moiety as a new radiolabeled vesamicol analog. We have previously reported the high potential of radioiodinated *o*-iodo-*trans*-decalinvesamicol (OIDV) and radiobrominated o-bromo-*trans*-decalinvesamicol (OBDV) as a VAChT ligand for SPECT and PET imaging, respectively [21–23]. However, the sensitivity, resolution and quantitative analysis of SPECT imaging are inferior to those of PET imaging. Radiobromine such as ^{76}Br, ^{77}Br as positron nuclide is not available commercially yet. Therefore, in the present study, we synthesized *o*-[^{11}C]methyl-*trans*-decalinvesamicol([^{11}C]OMDV), and evaluated both in vitro and in vivo in order to develop a new VAChT imaging ligand for PET.

Materials and methods

General

Vesamicol, (+)-pentazocine, and 1,3-di-*o*-tolylguanidine (DTG) were purchased from Sigma-Aldrich Co. (St. Louis, MO). Radioisotopes were purchased from PerkinElmer, Inc. (Waltham, MA), unless otherwise noted.

Animal experiments were performed in compliance with the Guidelines for the Care and Use of Laboratory Animals at the Takara-machi Campus of Kanazawa University.

Synthesis of OMDV

OMDV was synthesized from *o*-methylbenzaldehyde via the method previously described, except with the use of *o*-bromobenzaldehyde as the starting material [21]. Overall yield of OMDV from *o*-methylbenzaldehyde was 15 %.

Radiosynthesis and Isolation of [^{11}C]OMDV

[^{11}C]OMDV was prepared from *o*-trimethylstannyl-*trans*-decalinvesamicol (OTDV) (1.9 mg, 4.0 μmol), tris(dibenzylideneacetone)dipalladium(0) ($Pd_2(dba)_3$) (1.3 mg, 1.4 μmol), copper chloride (Cu(I)Cl) (0.28 mg, 0.27 μmol), cesium fluoride (CsF) (1.1 mg, 7 μmol), and tri(*o*-tol)phosphine ((o-tol)$_3$P) (6.5 mg, 22 μmol) by a palladium-promoted cross-coupling reaction using [^{11}C]methyl iodide [18, 24]. [^{11}C]OMDV was isolated using a reverse phase HPLC column (Waters XBridge Prep C18 (5 μm), 10 mm × 250 mm) with a mobile phase of acetonitrile/50 mM$AcONH_4$ in 0.1 % AcOH (45/55) at a flow rate of 6.0 mL/min (UV detector at 254 nm). The retention time of [^{11}C]OMDV was approximately 13 min. Isolated [^{11}C]OMDV was analyzed by HPLC using a YMC-Pac Pro C18 S-5 column (4.6 × 100 mm) with a mobile phase of acetonitrile/50 mM$AcONH_4$ in 0.1 % AcOH (45/55) at a flow rate of 1.2 mL/min (UV detector at 254 nm) to evaluate radiochemical purity and specific activity of [^{11}C]OMDV.

Tissue preparation

Rat brain and liver tissue preparations were prepared from dissected brains (not including the cerebellum) and livers from male Sprague-Dawley rats (250–300 g), as previously described [25].

In vitro competitive binding study

The following binding assays were performed using methods reported previously [25], and are described briefly here.

VAChT binding

(−)-[^{3}H]vesamicol (K_d = 7.40 nM) was used as a radioligand. Various concentrations of OMDV, DV benzovesamicol (BV), or vesamicol (from 10^{-10} to 10^{-5} M) were used as subject compounds. After addition of the compounds to the rat brain tissue preparation (300–400 μg protein), each sample was incubated at 37 °C for 60 min in the presence of 200 nM DTG to mask the sigma receptors (σ-1 and σ-2). Radioactivity retained on the filters after filtration of the samples was measured using a liquid scintillation counter (Aloka, LSC-5100).

σ-1 receptor binding

0.5 ml samples of 50 mM Tris–HCl (pH 7.8) including rat brain tissue preparation (400–500 μg protein), 5 nM (+)-[^{3}H]pentazocine (K_d = 19.9 nM), and various concentrations of OMDV, DV, BV, vesamicol, or sigma ligands (from 10^{-10} to 10^{-5} M) were incubated for 90 min at 37 °C. Nonspecific binding was determined in the presence of 10 μM (+)-pentazocine. After incubation, radioactivity retained on the filters after filtration of the samples was measured using a liquid scintillation counter (Aloka, LSC-5100).

σ-2 receptor binding

0.5 ml samples of 50 mM Tris–HCl (pH 7.8) including rat liver tissue preparation (approximately 100 μg protein), 5 nM [^{3}H]DTG (K_d = 22.3 nM), various concentrations of OMDV, DV, BV, vesamicol, or sigma ligands (from 10^{-10} to 10^{-5} M), and 1 μM (+)-pentazocine to mask the σ-1 sites were incubated for 90 min at 37 °C. Nonspecific binding was determined in the presence of 10 μM DTG and 1 μM (+)-pentazocine. The incubated samples were treated in the same manner as described for the σ-1 receptor binding assays.

Data analysis

K_i values were calculated using Graphpad Prism (GraphPad Software, Inc. San Diego, USA).

Biodistribution study

[^{11}C]OMDV (0.4 mL, 37–105 MBq) was injected intravenously in four groups of male Sprague-Dawley (SD) rats (250–300 g, n = 4 in each group). At 2, 10, 30, and 60 min post-injection, the animals were killed immediately by decapitation. The organs of interest were dissected and weighed, and the radioactivity levels were measured in a gamma scintillation counter (Wallac Wizard 3, Perkin Elmer, USA). The accumulation of radiotracer was expressed as a percentage of the administered dose per gram of tissue (% ID/g). Using this method, the regional brain distribution (cortex, striatum, cerebellum, and the rest of the brain) of [^{11}C]OMDV (0.4 mL, 5.2 MBq) 30 min post-injection was determined.

In vivo blocking study

Four groups of male SD rats (250–300 g, n = 4 in each group) received an intravenous injection of [^{11}C]OMDV (3–27 MBq) either with or without (control) 0.125 or 0.250 μmol vesamicol, 0.125 μmol (+)-pentazocine, and 0.125 μmol (+)-3-(3-hydroxyphenyl)-N-propylpiperidine ((+)-3-PPP). The rats were killed 30 min after injection and their brains were collected. Each dissected brain was divided into four regions: the cortex, striatum, cerebellum and the remainder of brain, and the weight and radioactivity of each portion was measured.

PET measurement in the rat brain

SD rats were immobilized on a PET–CT camera, (model FX3000, Gamma Medica-Ideas, USA), and injected intravenously with [^{11}C]OMDV (0.4 mL, 45 MBq) either with or without 0.250 μmol vesamicol via the tail vein. PET scanning was performed for 40 min with the first 6 frames at 20 s intervals, followed by 5 frames at 60 s intervals, 4 frames at 2 min intervals, and finally 5 frames at 5 min intervals. Regions of interest (ROIs) were centered on the cerebrum and time–activity curves in the ROIs were obtained. Decay-corrected radioactivity was expressed as the standardized uptake value (SUV). The differences in brain uptake between rats administered 0.25 μmol vesamicol and control rats were calculated using the mean SUV acquired for 5 min, 25 min after tracer injection.

Statistical analysis

In the in vivo blocking study, statistical comparisons were performed using one-way ANOVA (non-parametric), and Tukey's multiple comparison test (GraphPad Prism Version 4 software).

Results

In vitro competitive binding study

Binding affinity (K_i) of OMDV, DV, BV, vesamicol and the sigma ligands to the VAChT binding sites and sigma receptors (σ-1, σ-2) are shown in Table 1. OMDV (11.9 nM) as well as DV (10.6 nM) and BV (11.8 nM) showed a higher binding affinity for VAChT than vesamicol (21.1 nM). OMDV as well as DV showed a lower binding affinity for σ-1 receptor than vesamicol and BV. However, OMDV showed a higher affinity for σ-2 receptor than vesamicol and BV.

Radiolabeling of [^{11}C]OMDV

[^{11}C]OMDV was radiolabeled by methylation of *o*-trimethylstannyl-*trans*-decalinvesamicol (OTDV) with [^{11}C]methyl iodide in a palladium-promoted cross-coupling reaction (Fig. 1) [18]. The total synthesis time was approximately 30 min. The decay-corrected radiochemical yield was 60–75 %, calculated using radioactivity of [^{11}C]methyl iodide, and the radiochemical purity determined by analytical

Table 1 Binding affinities of vesamicol, BV, DV, and OMDV for VAChT and the σ-1 and σ-2 receptors

Compounds	K_i (nM)		
	VAChT	σ-1	σ-2
OMDV	11.9	70.3	43.6
DV	10.6	57.3	46.8
BV	11.8	16.7	120
(±)-vesamicol	21.1	20.8	139
(+)-pentazocine	–	8.7	1803
DTG	–	90.9	27.6

$K_i = IC_{50}$ $(1 + C/K_d)$, C Concentration of radioligand

Values are the mean ± standard deviation

HPLC was >98 %. The specific activity was 5–10 TBq/mmol 30 min after the end of bombardment (EOB).

In vivo biodistribution

Table 2 shows the tissue distribution of [^{11}C]OMDV at 2, 10, 30, and 60 min post-injection. At 2 min post-injection, [^{11}C]OMDV showed relatively high accumulation in the cerebrum (0.92 ± 0.09) and cerebellum (0.73 ± 0.09), presumably after [^{11}C]OMDV passage through the blood–brain barrier (BBB). At 10 and 30 min post-injection, [^{11}C]OMDV accumulation in the cerebrum remained stable (0.71 ± 0.10 and 0.65 ± 0.07, respectively), and [^{11}C]OMDV accumulation in the cerebrum was consistently higher than that in the cerebellum (0.53 ± 0.07 and 0.52 ± 0.07, respectively). [^{11}C]OMDV accumulation in the blood (0.11 ± 0.01) was quite low even 2 min post-injection. [^{11}C]OMDV accumulation in the lung, heart and kidney was highest 2 min post-injection. [^{11}C]OMDV accumulation in many tissues, such as the pancreas, spleen, small intestines, stomach and liver, were highest at more than 30 min after injection.

Table 3 shows the regional brain distribution of [^{11}C]OMDV 30 min post-injection. [^{11}C]OMDV accumulation was highest in the striatum (0.69 ± 0.12 %ID/g), followed by the cortex (0.62 ± 0.10), the rest of the brain (0.62 ± 0.11), and the cerebellum (0.50 ± 0.10). [^{11}C]OMDV accumulation in the striatum was highest among interest brain regions.

In vivo blocking study

To estimate the binding selectivity of [^{11}C]OMDV to VAChT in vivo, we studied the blocking ability of three

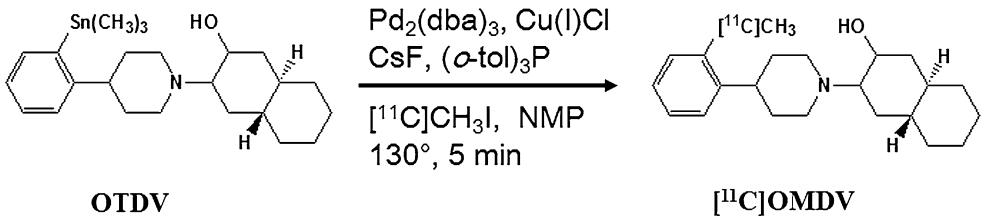

OTDV **[^{11}C]OMDV**

Fig. 1 Radiosynthesis of [^{11}C]OMDV

Table 2 Biodistribution of [^{11}C]OMDV in rats

Organs	[^{11}C]OMDV			
	% ID/g			
	Time post-injection			
	2 min	10 min	30 min	60 min
Blood	0.11 ± 0.01	0.06 ± 0.00	0.05 ± 0.00	0.03 ± 0.00
Heart	1.73 ± 0.25	0.43 ± 0.08	0.30 ± 0.04	0.17 ± 0.01
Lung	4.84 ± 1.48	2.05 ± 0.68	1.21 ± 0.39	0.82 ± 0.09
Pancreas	1.90 ± 0.26	2.52 ± 0.57	2.78 ± 0.21	3.01 ± 0.52
Spleen	0.78 ± 0.32	1.17 ± 0.35	1.25 ± 0.12	0.89 ± 0.06
Kidney	2.60 ± 0.40	1.70 ± 0.23	1.90 ± 0.38	1.52 ± 0.21
Small intestines	0.97 ± 0.27	1.45 ± 0.35	1.88 ± 0.82	2.23 ± 0.68
Stomach	0.28 ± 0.21	0.39 ± 0.09	1.16 ± 0.29	0.43 ± 0.22
Liver	1.15 ± 0.29	1.49 ± 0.46	2.02 ± 0.22	2.01 ± 0.45
Cerebrum	0.92 ± 0.09	0.71 ± 0.10	0.65 ± 0.07	0.44 ± 0.06
Cerebellum	0.73 ± 0.09	0.53 ± 0.07	0.52 ± 0.07	0.35 ± 0.05

Values are the mean ± standard deviation (SD) of four rats ($n = 4$) at each time point

Table 3 Regional rat brain distribution of [^{11}C]OMDV 30 min post-injection

Organs	[^{11}C]OMDV % ID/g
Blood	0.03 ± 0.00
Cortex	0.62 ± 0.10
Striatum	0.69 ± 0.12
Cerebellum	0.50 ± 0.10
Rest of the brain	0.62 ± 0.11

Values are the mean ± standard deviation (SD) of four rats ($n = 4$)

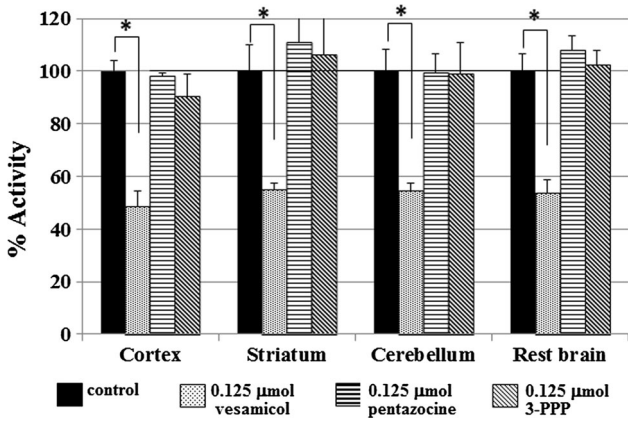

Fig. 2 Inhibition of [^{11}C]OMDV accumulation in the cortex, striatum, cerebellum, and the rest of the brain by co-administration of vesamicol, pentazocine and 3-PPP. A one-way ANOVA followed by a Tukey's multiple comparison test was performed by GraphPad Prism Version 4 software, compared with the control. * $P < 0.05$

agents [vesamicol (VAChT ligand), pentazocine (σ-1 receptor ligand) or (+)-3-PPP (σ-1, σ-2 receptor ligand)] on the regional brain uptake of [^{11}C]OMDV (Fig. 2). The uptake of [^{11}C]OMDV (about 45–50 % of control) was remarkably decreased in all four brain regions investigated when co-administered with 0.125 µmol vesamicol. On the other hand, no significant changes in [^{11}C]OMDV accumulation in any of the brain regions was observed with the co-administration of 0.125 µmol (+)-pentazocine or 0.125 µmol (+)-3-PPP. The inhibition of [^{11}C]OMDV accumulation in the four brain regions was more pronounced by co-administration of 0.250 µmol vesamicol (about 60 % of control) than by co-administration of 0.125 µmol vesamicol (about 40 % of control) (Fig. 3).

PET measurement in the rat brain

Figure 4 shows PET–CT fusion brain images after [^{11}C]OMDV administration in rats. The accumulation of [^{11}C]OMDV in the brain was remarkably decreased by co-administration of 0.250 µmol vesamicol. Figure 5 shows

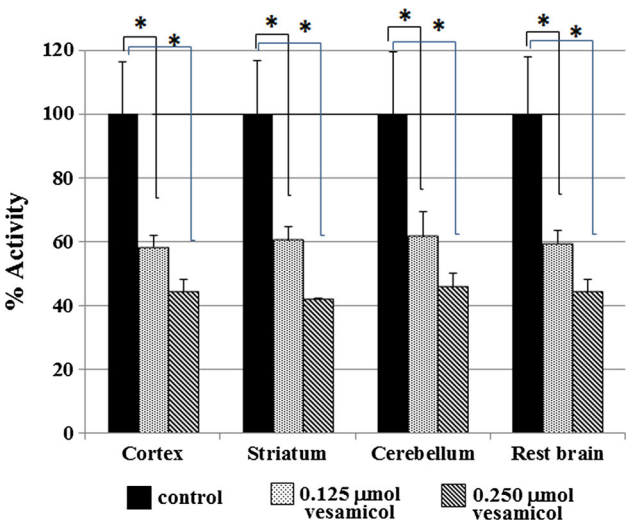

Fig. 3 Inhibition of [^{11}C]OMDV accumulation by co-administration of vesamicol (0.125 or 0.250 µmol). A one-way ANOVA followed by a Tukey's multiple comparison test was performed by GraphPad Prism Version 4 software, compared with the control. * $P < 0.05$

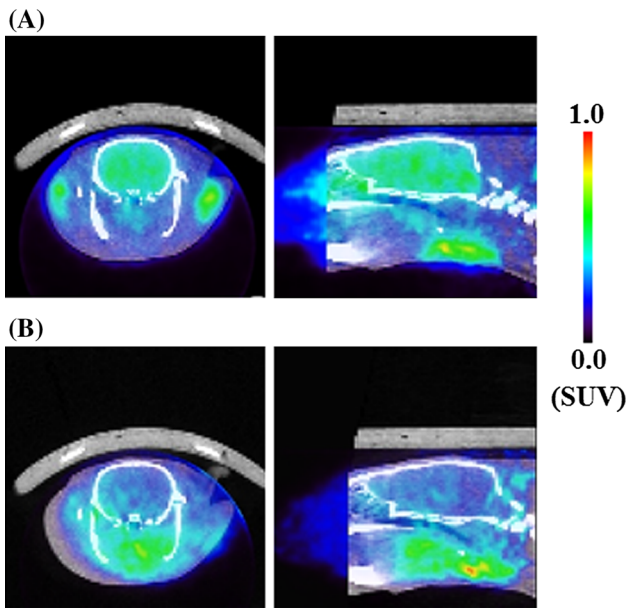

Fig. 4 PET–CT fusion brain images with [^{11}C]OMDV alone (**a**); or with 0.250 µmol vesamicol as an inhibitor (**b**). Images were acquired for 5 min starting 28 min after tracer injection

the time–activity curves of each brain region after administration of [^{11}C]OMDV alone (A) and [^{11}C]OMDV co-administered with 0.250 µmol vesamicol (B). No differences were observed in the initial uptake (SUV) of [^{11}C]OMDV when administered alone (A) or with 0.250 µmol vesamicol (B). However, clearance of [^{11}C]OMDV accumulation when co-administrated with 0.250 µmol vesamicol (B) was faster than when administered alone (A).

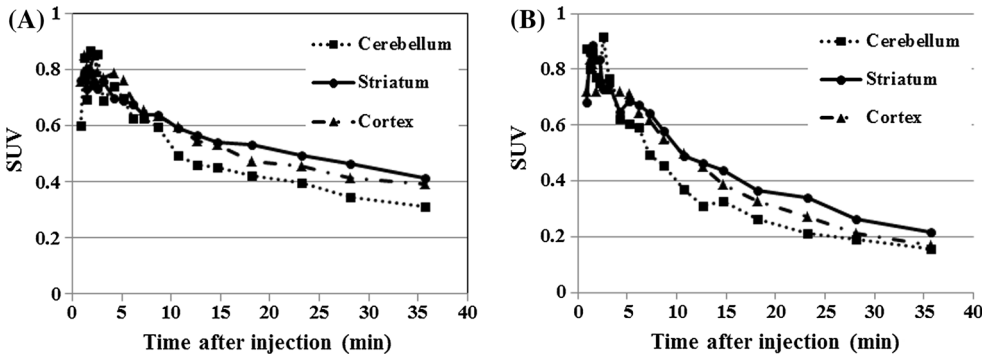

Fig. 5 Typical time–activity curves in different rat brain regions of [^{11}C]OMDV alone (**a**); or with 0.250 μmol vesamicol as an inhibitor (**b**). Radioactivity levels are expressed as the standardized uptake value (SUV)

Discussion

[^{11}C]OMDV was synthesized by a palladium-promoted cross-coupling reaction with [^{11}C]methyl iodide [18, 24]. [^{11}C]OMDV was prepared with a sufficient radiochemical yield (60–75 %), and greater than 98 % radiochemical purity for use in the in vivo studies. The specific radioactivity was 5–10 TBq/mmol 30 min after EOB. The low specific radioactivity may be explained by possible cross-coupling between one of the methyl groups on the tin and the nucleoside part, yielding OMDV [26].

In the in vitro competitive binding study, OMDV binding affinity ratio of VAChT to the σ-1 and σ-2 receptors was 5.9 and 3.7, respectively, and the vesamicol binding affinity ratio of VAChT to the σ-1 and σ-2 receptors was 0.99 and 6.6, respectively, suggesting the binding selectivity of OMDV for VAChT was higher than that of vesamicol. Following OMDV showed not only a higher binding affinity but also a higher binding selectivity for VAChT than vesamicol in vitro. BV had a high binding affinity for both VAChT (11.8 nM) and the σ-1 receptor (16.7 nM), indicating BV had a lower selectivity for VAChT compared to DV.

The brain uptake of [^{11}C]OMDV(0.65 %ID/g) 30 min post-injection was approximately 1.5 times higher than that of [^{125}I]OIDV (0.42 %ID/g), a VAChT imaging probe for SPECT previously reported [22]. Therefore, the high brain accumulation of [^{11}C]OMDV may be advantageous for its in vivo visualization of brain.

Accumulation of [^{11}C]OMDV 30 min post-injection was highest in the striatum (0.69 ± 0.12), followed by the cortex (0.62 ± 0.10) and cerebellum (0.50 ± 0.10), in confirmation with the known distribution of high VAChT density in the striatum [27, 28].

Initial blood accumulation of [^{11}C]OMDV 2 min post-injection was low (0.11 ± 0.01 % ID/g), and its clearance from the blood was fast, with radioactivity detected in the blood at 0.03 ± 0.00 % ID/g 60 min post-injection. This low accumulation in the blood and rapid clearance are advantageous for brain imaging. The metabolic process of [^{11}C]OMDV may be similar to that of [^{125}I]OIDV, due to similar time-course distributions in the blood, heart, lung, pancreas, kidney, stomach, and small intestine [22].

The blocking effect of vesamicol on uptake of [^{11}C]OMDV in the brain was dose-dependent; however, the blocking effect of vesamicol was not better than expected, which showed that the ratio of nonspecific uptake to specific uptake of [^{11}C]OMDV in brain was not good in comparison with that of [^{125}I]OIDV. Brain uptake of [^{11}C]OMDV did not significantly alter by co-administration of sigma receptor ligands ((+)-pentazocine or 3-PPP), indicating selective [^{11}C]OMDV binding to VAChT in vivo.

PET imaging of the rat brain demonstrated that the uptake of [^{11}C]OMDV was relatively higher in the striatum (Fig. 5), likely due to the high expression of VAChT [28] and low expression of the σ-1 [29]. These data suggest that, due to its binding to VAChT, the use of [^{11}C]OMDV may contribute to improved PET imaging of the striatum.

The specific binding of [^{11}C]OMDV to VAChT was further confirmed by observing the decrease of brain accumulation of [^{11}C]OMDV by co-administration of vesamicol by PET–CT. However, [^{11}C]OMDV was observed to be accumulated throughout the rat brain; previous reports [23] have suggested that the expression pattern of VAChT, which was localized to the presynaptic terminals of the cholinergic nervous system, was similar to those of the muscarinic acetylcholine receptors (M_1–M_5) [30–33] and nicotinic receptor [34]. Expressions of VAChT in brain were characterized by higher concentration of VAChT in striatum than cerebral cortex, by regional brain distribution of VAChT imaging ligands and [^{3}H]vesamicol in in vivo or in vitro [16, 35, 36]. On the other hand, expressions of sigma receptors in brain were characterized by higher concentration of sigma receptors in cerebral cortex than striatum [37–39]. [^{11}C]OMDV accumulated at higher concentration in striatum than cerebral cortex in vivo, which showed that [^{11}C]OMDV bound to VAChT in brain in vivo. Because cholinergic neurons in cerebral cortex belong to projection neurons which the

basal forebrain cholinergic neuron complex such as the nucleus basalis of Meynert (NMB) [40–42], the medial septal nucleus and the diagonal band nuclei projects to, and the function of cerebral cortex is associated with a cognitive, learning and memory functions, VAChT in cerebral cortex will be suitable to the target for early diagnosis of Alzheimer's disease. On the other hand, because cholinergic neurons in striatum consist of local circuit cells, which means a nerve signal is transmitted only in striatum, cholinergic neurons in striatum are not necessarily related to cognitive impairment in Alzheimer's disease.

Conclusion

OMDV demonstrated high binding affinity to VAChT in vitro; however, binding selectivity of OMDV to VAChT was inferior to that of OIDV or OBDV a little. In vivo, [^{11}C]OMDV was accumulated in regions of the rat brain reflecting areas of high VAChT expression. Use of [^{11}C]OMDV may be suitable as a radioligand for PET in the study of dementia, which is characterized by degeneration of the cholinergic neurotransmitter system.

Acknowledgments The authors would like to thank Ms. Miyuki Nakashima for her assistance with the in vitro and in vivo experiments. This work was supported by a Grant-in-Aid for Scientific Research (B) (No. 26293273) from the Ministry of Education, Culture, Sports, Science and Technology of Japan.

References

1. Mohs RC, Doody RS, Morris JC, Ieni JR, Rogers SL, Perdomo CA, et al. A 1-year, placebo-controlled preservation of function survival study of donepezil. Neurology. 2001;57:481–8.
2. Gauthier S, Lopez OL, Waldermar G, Lones RW, Cummings J, Zhang R, et al. Effects of donepezil on activities of daily living: integrated analysis of patient data from studies in mild, moderate and severe Alzheimer's disease. Int Psychogeriatr. 2010;22: 973–83.
3. McGeer PL. Aging, Alzheimer's disease, and the cholinergic system. Can J Physiol Pharmacol. 1984;62:741–54.
4. Reinikainen KJ, Soininen H, Riekkinen PJ. Neurotransmitter changes in Alzheimer's disease: implications to diagnostics. J Neurosci Res. 1990;27:576–86.
5. Efange SM, Garland EM, Staley JK, Khare AB, Mash DC. Vesicular acetylcholine transporter density and Alzheimer's disease. Neurobiol Aging. 1997;18(4):407–13.
6. Kuhl DE, Minoshima S, Fessler JA, Frey KA, Foster NL, Ficaro EP, et al. In vivo mapping of cholinergic terminals in normal aging, Alzheimer's disease, and Parkinson's disease. Annals of neurology. 1996;40(3):399–410.
7. Prado VF, Martins-Silva C, de Castro BM, Lima RF, Barros DM, Amaral E, et al. Mice deficient for the vesicular acetylcholine transporter are myasthenic and have deficits in object and social recognition. Neuron. 2006;51(5):601–12.
8. Schafer MK, Weihe E, Erickson JD, Eiden LE. Human and monkey cholinergic neurons visualized in paraffin-embedded tissues by immunoreactivity for VAChT, the vesicular acetylcholine transporter. J Mol Neurosci. 1995;6:225–35.
9. Yoshiyama Y, Higuchi M, Zhang B, et al. Synapse loss and microglial activation precede tangles in a P 301 S tauopathy mouse model. Neuron. 2007;53:337–51.
10. Bar BA, Parsons SM. Demonstration of a receptor in Torpedo synaptic vesicles for the acetylcholine storage blocker L-trans-2-(4-phenyl[3,4-^{3}H]-piperidino) cyclohexanol. Proc Natl Acad Sci USA. 1986;83:2267–70.
11. Marshall IG, Parsons SM. The vesicular acetylcholine transport system. TINS. 1987;10:174–7.
12. Prado VF, Martins-Silva C, de Castro BM, Lima RF, Barros DM, Amaral E, et al. Mice deficient for the vesicular acetylcholine transporter are myasthenic and have deficits in object and social recognition. Neuron. 2006;51(5):601–12.
13. Efange SM, Michelson RH, Khare AB, Thomas JR. Synthesis and tissue distribution of (m-[^{125}I]iodobenzyl)trozamicol ([^{125}I]MIBT): potential radioligand for mapping central cholinergic innervation. J Med Chem. 1993;36:1754–60.
14. Efange SM, Mach RH, Khare AB, Michelson RH, Nowak PA, Evora PH. [^{18}F]Fluorobenzyltrozamicol ([^{18}F]FBT): molecular decomposition-reconstitution approach to vesamicol receptor radioligands for positron emission tomography. Appl Radiat Isot. 1994;45:465–72.
15. Mulholland GK, Wieland DM, Kilbourn MR, Frey KA, Sherman PS, Carey JE, et al. [^{18}F]Fluoroethoxy-benzovesamicol, a PET radiotracer for the vesicular acetylcholine transporter and cholinergic synapses. Synapse. 1998;30:263–74.
16. Sorger D, Schliebs R, Kampfer I, Rossner S, Heinicke J, Dannenberg C, et al. In Vivo [^{125}I]-Iodobenzovesamicol binding reflects cortical cholinergic deficiency induced by specific immunolesion of rat basal forebrain cholinergic system. Nucl Med Biol. 2000;27:23–31.
17. Shiba K, Mori H, Tonami N. Evaluation of radioiodinated (−)-*o*-iodovesamicol as a radiotracer for mapping the vesicular acetylcholine transporter. Ann Nucl Med. 2003;17(6):451–6.
18. Shiba K, Nishiyama S, Tsukada H, Ishiwata K, Kawamura K, Ogawa K, et al. The potential of (−)-*o*-[^{11}C]methylvesamicol for diagnosing cholinergic deficit dementia. Synapse. 2009;63(2):167–71.
19. Efange SM, Mach RH, Smith CR, Khare AB, Foulon C, Akella SK, et al. Vesamicol analogues as sigma ligands: molecular determinants of selectivity at the vesamicol receptor. Biochem Pharmacol. 1995;49:791–7.
20. Rogers GA, Parsons SM, Anderson DC, Nilsson LM, Bahr BA, Kornreich WD, et al. Synthesis, in vitro acetylcholine- storage-blocking activities, and biological properties of derivatives and analogues of trans-2-(4-phenylpiperidineo) cyclohexanol (Vesamicol). J Med Chem. 1989;32:1217–30.
21. Kozaka T, Uno I, Kitamura Y, Miwa D, Ogawa K, Shiba K. Syntheses and in vitro evaluation of decalinvesamicol analogues as potential imaging probes for vesicular acetylcholine transporter (VAChT). Bioorg Med Chem. 2012;20(16):4936–41.
22. Kozaka T, Uno I, Kitamura Y, Miwa D, Azim MA, Ogawa K, et al. Regional brain imaging of vesicular acetylcholine transporter (VAChT) using *o*-[^{125}I]iodo-*trans*-decalinvesamicol as a new potential imaging probe. Synapse. 2014;68(3):107–13.
23. Azim MA, Kozaka T, Uno I, Miwa D, Kitamura Y, Ogawa K, et al. The potential of the vesicular acetylcholine transporter (VAChT) Imaging Using Radiolabeled *o*-Bromo-*trans*-decalinvesamicol (OBDV) as a New PET Ligand. Synapse. 2014;68: 445–53.
24. Kawamura K, Shiba K, Tsukada H, Nishimura S, Mori H, Ishiwata K. Synthesis and evaluation of vesamicol analog (−)-*o*-[^{11}C]methylvesamicol as a PET ligand for vasicular acetylcholine transporter. Annal. Nucl. Med. 2006;20(6):417–24.

25. Shiba K, Yano T, Sato W, Mori H, Tonami N. Characterization of radioiodinated (−)-ortho-iodovesamicol binding in rat brain preparations. Life Sci. 2002;71(13):1591–8.
26. Samuelsson L, Långström B. Synthesis of 1-(2′-deoxy-2′-fluoro-β-D-arabinofuranosyl)-[methyl-^{11}C]thimine ([^{11}C]FMAU) via a still cross-coupling reaction with [^{11}C]methyl iodide. J Label Compd Radiopharm. 2003;46:263–72.
27. Frey KA, Wieland DM, Kilbourn MR. Imaging of monoaminergic and cholinergic vesicular transporters in the brain. Adv Pharmacol. 1998;42:269–72.
28. Efange SM. In vivo imaging of the vesicular acetylcholine transporter and the vesicular monoamine transporter. FASEB J. 2000;14:2401–13.
29. Mash DC, Zabetian CP. Sigma receptors are associated with cortical limbic areas in the primate brain. Synapse. 1992;12: 195–205.
30. David A, McCormick. 1989, Acetylcholine: distribution, receptors, and actions. Section of Neuroanatomy, Yale Univrersity of School of Medicine. 333 Cedar Street, New Haven, CT 06510, USA.
31. Quirion R, Aubert I, Araujo DM, Hersi A, Gaudreau P. Autoradiographic distribution of putative muscarinic receptor sub-types in mammalian brain. Prog Brain Res. 1993;98:85–93.
32. Levey AI, Kitt CA, Simonds WF, Price DL, Brann MR. Identification and localization of muscarinic acetylcholine receptor proteins in brain with subtype-specific antibodies. The Journal of Neuroscience. 1991;11(10):3218–26.
33. Vilaro MT, Mengod G, Palacios JM. Advances and limitations of the molecular neuroanatomy of cholinergic receptors: the example of multiple muscarinic receptors. Prog Brain Res. 1993;98: 95–101.
34. Rotter A, Jacobwitz DM. Neurochemical identification of cholinergic forebrain projection sites of the nucleus tegmentalis dorsalis lateralis. Brain Res Bull. 1981;6:525–9.
35. Jung YW, Van Dort ME, Gildersleeve DL, Wieland DM. A radiotracer for mapping cholinergic neurons of the brain. J Med Chem. 1990;33:2065–8.
36. Altar CA, Marien MR. [^{3}H]vesamicol binding in brain: autoradiographic distribution, pharmacology, and effects of cholinergic lesions. Synapse. 1988;2(5):486–93.
37. Weissman AD, Su T-P, Hedreen JC, London ED. Sigma receptors in post-mortem human brains. J Pharmacol Exp Ther. 1988;247(1):29–33.
38. Waterhouse RN, Mardon K, O'Brien JC. Synthesis and Preliminary Evaluation of [^{123}I]1-(4-Cyanobenzyl)-4-[[(trans-iodopropen-2-yl)oxy]-methyl]piperidine: a novel high affinity sigma receptor radioligand for SPECT. Nucl Med Biol. 1997;24:45–51.
39. Kawamura K, Ishiwata K, Tajima H, Ishii S. In vivo evaluation of [^{11}C]SA4503 as a PET Ligand for mapping CNS sigma1 receptor. Nucl Med Biol. 2000;27:255–61.
40. Butcher LL, Oh JD, Woolf NJ. Cholinergic neurons identified by in situ hybridization histochemistry. Prog Brain Res. 1993; 98:1–8.
41. Woolf NJ, Eckenstein F, Butcher LL. Cholinergic projections from the basal forebrain to the frontal cortex: a combined fluorescent tracer and immunohistochemical analysis. Neurosci Lett. 1983;40:93–8.
42. Woolf NJ, Butcher LL. Cholinergic system in the rat brain: III. Projection from the pontomesencephalic tegmentum to the thalamus, tectum, basal ganglia, and basal forebrain. Brain Res Bull. 1986;16:603–37.